AD-A069 106 ARMY ARMAMENT RESEARCH AND DEVELOPMENT COMMAND ABERD--ETC F/G 19/4
COMPUTATION OF TRANSONIC FLOW PAST PROJECTILES AT ANGLE OF ATTA--ETC(U)
FEB 79 R P REKLIS, W B STUREK, F R BAILEY

UNCLASSIFIED ARBRL-TR-02139 SBIE-AD-E430 233 NL

| OF |
AD
A069106

END
DATE
FILMED
6-79
DDC

TECHNICAL REPORT ARBRL-TR-02139

COMPUTATION OF TRANSONIC FLOW PAST PROJECTILES AT ANGLE OF ATTACK

R. P. Reklis
W. B. Sturek
F. R. Bailey

February 1979

US ARMY ARMAMENT RESEARCH AND DEVELOPMENT COMMAND
BALLISTIC RESEARCH LABORATORY
ABERDEEN PROVING GROUND, MARYLAND

Destroy this report when it is no longer needed.
Do not return it to the originator.

Secondary distribution of this report by originating or sponsoring activity is prohibited.

Additional copies of this report may be obtained from the National Technical Information Service, U.S. Department of Commerce, Springfield, Virginia 22161.

The findings in this report are not to be construed as an official Department of the Army position, unless so designated by other authorized documents.

The use of trade names or manufacturers' names in this report does not constitute indorsement of any commercial product.

UNCLASSIFIED

SECURITY CLASSIFICATION OF THIS PAGE (When Data Entered)

REPORT DOCUMENTATION PAGE

READ INSTRUCTIONS BEFORE COMPLETING FORM

1. REPORT NUMBER: TECHNICAL REPORT ARBRL-TR-02139	2. GOVT ACCESSION NO. / 3. RECIPIENT'S CATALOG NUMBER
4. TITLE (and Subtitle): COMPUTATION OF TRANSONIC FLOW PAST PROJECTILES AT ANGLE OF ATTACK	5. TYPE OF REPORT & PERIOD COVERED: Final 6. PERFORMING ORG. REPORT NUMBER
7. AUTHOR(s): R. P. Reklis, W. B. Sturek, F. R. Bailey	8. CONTRACT OR GRANT NUMBER(s)
9. PERFORMING ORGANIZATION NAME AND ADDRESS: U.S. Army Ballistic Research Laboratory (ATTN: DRDAR-BLL) Aberdeen Proving Ground, Maryland 21005	10. PROGRAM ELEMENT, PROJECT, TASK AREA & WORK UNIT NUMBERS: RDT&E 1L161102AH43
11. CONTROLLING OFFICE NAME AND ADDRESS: U.S. Army Armament Research & Development Command, U.S. Army Ballistic Research Laboratory (ATTN: DRDAR-BL) Aberdeen Proving Ground, MD 21005	12. REPORT DATE: FEBRUARY 1979 13. NUMBER OF PAGES: 30
14. MONITORING AGENCY NAME & ADDRESS (if different from Controlling Office)	15. SECURITY CLASS. (of this report): Unclassified 15a. DECLASSIFICATION/DOWNGRADING SCHEDULE

16. DISTRIBUTION STATEMENT (of this Report)

Approved for public release; distribution unlimited.

17. DISTRIBUTION STATEMENT (of the abstract entered in Block 20, if different from Report)

18. SUPPLEMENTARY NOTES

19. KEY WORDS (Continue on reverse side if necessary and identify by block number)

Transonic Flow
Inviscid Flow
Three-Dimensional Flow
Projectile Aerodynamics
Computational Fluid Dynamics
Spectral Techniques

20. ABSTRACT (Continue on reverse side if necessary and identify by block number) (1cb)

Aerodynamic properties of artillery shell such as normal force and pitching moment reach peak values in a narrow transonic Mach number range. In order to compute these quantities, numerical techniques have been developed to obtain solutions to the three-dimensional transonic small disturbance equation about slender bodies at angle of attack. The computation is based on a plane relaxation technique involving Fourier transforms to partially decouple the three-dimensional difference equations. Particular care is taken to assure accurate

(Continued)

DD FORM 1 JAN 73 1473 EDITION OF 1 NOV 65 IS OBSOLETE

UNCLASSIFIED

SECURITY CLASSIFICATION OF THIS PAGE (When Data Entered)

20. ABSTRACT (Continued):

solutions near corners found in shell designs. Computed surface pressures are compared to experimental measurements for circular arc and cone cylinder bodies which have been selected as test cases. Computed pitching moments are compared to range measurements for a typical projectile shape.

TABLE OF CONTENTS

LIST OF ILLUSTRATIONS

I. INTRODUCTION

When designing an artillery shell, it is necessary to develop a vehicle which will fly with stability under a wide variety of aerodynamic conditions. A range of propellant charges may be used giving the shell launch velocities covering a spectrum from subsonic to supersonic. The shell will also slow in flight, particularly near the apex of its trajectory. It is, therefore, important that the shell fly with stability in subsonic, transonic, and supersonic flight regimes.

Difficulties are often experienced by projectiles at transonic velocities. Aerodynamic properties such as drag and the pitching moment, which is critical to stability, will reach peak values at some transonic Mach number. This peak can form in a Mach number range which may be limited, for example, between $.92 < M < .94$. The sharpness of this critical behavior as well as the value of the critical Mach number are very sensitive to body geometry. A slight change in boattail length may make the difference between a successful shell and one whose behavior is unpredictable.

Aerodynamic range and wind tunnel testing are difficult and expensive, particularly at transonic velocities. Therefore, it is of great importance for artillery projectile design to develop a computational capability which can provide guidance in the design of shell configurations and reduce aerodynamic testing requirements. Techniques have been established[1] and computers are now available which should make possible the development of useful computational design tools, particularly for the limited and seemingly simple geometries found in artillery projectile shapes. The techniques presented here will treat inviscid transonic flow over projectiles allowing the computation of lift and pitching moment. Magnus effects will be included in following work when viscous effects are included.

The simplicity of the shape of an artillery shell is somewhat deceptive. There are sharp corners and other discontinuities in the surface slope and curvature. These discontinuities create strong shock patterns at transonic velocities as may be seen in the shadowgraph presented in Figure 1. An understanding of these shock patterns is critical to an understanding of the aerodynamics of the shell. The shock on the windward surface of the boattail is a great deal farther aft than the shock on the lee surface. This pattern generates a strong upward force on the boattail tending to overturn the shell and thus generates a large pitching moment.

---

1. *F. R. Bailey and W. F. Ballhaus, "Comparisons of Computed and Experimental Pressures for Transonic Flow About Isolated Wings and Wing Fuselage Configurations," NASA SP-347, Vol. 2, March 1975, pp. 1213-1226.*

The resolution of the shock patterns associated with flow over the corners, makes necessary the application of very fine grids in the numerical procedures used to obtain predictions of the flow over the shell. The necessity of making three-dimensional computations with these fine grids leads to the problem of a large computer storage requirement and to the problem of a long run time. Grids on the order of ten thousand total points have been needed in two dimensions to suitably resolve the shock patterns and corner flows associated with shell. Computer time for such a solution based on a line relaxation scheme is close to one minute on a CDC 7600. A carry-over of the two-dimensional solution to three dimensions using line relaxation techniques could multiply time and storage requirements by a factor of 30. Such a computation time would be unacceptably long for engineering design purposes. Techniques suited to cylindrical problems in three dimensions will be developed in this paper which require about four times the effort necessary for a two-dimensional solution. This effort leads to a run time of about three minutes on the 7600 which is considered to be suitable for engineering use.

II. THE TRANSONIC SMALL DISTURBANCE EQUATION

The approach used here to compute transonic flow is based on the solution of the transonic small disturbance equation,

$$[1 - M^2 - M^2(\gamma+1)\phi_z]\phi_{zz} + \phi_{rr} + \phi_r/r + \phi_{\theta\theta}/r^2 = 0 \qquad (1)$$

which may be derived from the Euler equations applied to a slender body with a pointed nose[2]. The solution of this equation is the potential ϕ from which velocities and pressures in the flow field may be obtained. This is a non-linear partial differential equation of mixed elliptic-hyperbolic type written in a cylindrical coordinate system (z,r,θ) as shown in Figure 2. The free stream Mach number is given by M in this equation and the ratio of specific heats (1.4 for air) is represented by γ. Boundary conditions are given on the surface and at infinity by:

$$\phi_r\Big|_{\text{surface}} = dR/dz$$

and

$$\phi_\infty = \alpha\cos(\theta) \quad .$$

In these equations R is the radius of the surface and α is the angle of attack of the projectile.

---

2. *Holt Ashley and Marten Landahl, Aerodynamics of Wings and Bodies, Addison-Wesley Publishing, Inc., Reading, MA (1965).*

In practice it is more convenient to use a set of boundary conditions in which all the important information appears in the body surface equation, thus leaving the boundary condition at infinity as,

$$\phi_\infty = 0 \quad .$$

This desired arrangement of the boundary conditions may be accomplished by the transformation,

$$\phi = \nu + \alpha\, r \cos(\theta) \quad ,$$

$$\nu = \phi - \alpha\, r \cos(\theta) \quad .$$

This transformation does not alter the differential equation that must be solved. It does alter the boundary conditions, however, producing the new set:

$$\nu_r\Big|_{\text{surface}} = dR/dz - \alpha \cos(\theta) \quad ,$$

and

$$\nu_\infty = 0 \quad .$$

The solution to equation (1) has been shown by Bailey[3] to give good results for the slender body case at zero angle of attack. This equation has also been studied both numerically and analytically for many years and it is simple enough that much valuable insight may be gained from it.

III. FOURIER TRANSFORMATIONS

An examination of the closely related linear equation produced by holding the coefficient of ϕ_{zz} constant will demonstrate a technique for simplifying the solution of the three-dimensional problem. The equation that results from this linearization is

$$\lambda\phi_{zz} + \phi_{rr} + \phi_r/r + \phi_{\theta\theta}/r^2 = 0 \quad ,$$

---

3. *F. R. Bailey, "Numerical Calculation of Transonic Flow About Slender Bodies of Revolution," NASA TN-D-6582, December 1971.*

where λ is the constant coefficient. This equation is of the form that would be obtained from a strictly subsonic or supersonic problem in which the Mach number is well away from one. It is not necessary to resort to numerical techniques to solve this linearized equation. Ordinary analysis may be applied. As the problem is periodic in θ a Fourier transformation is a logical step. Such a transformation results when the potential is expanded in a cosine series in θ, as given by,

$$\phi\ (z,r,\theta) = \xi^{o}\ (z,r) + \xi^{1}\ (z,r) \cos\ (\theta) + \xi^{2}\ (z,r) \cos\ (2\theta) + \ldots$$

A two-dimensional differential equation may then be obtained for each coefficient ξ^{k}. Fortunately, because of the boundary conditions, only two of these coefficients are non-zero. The net result is the transformation of the original linear three-dimensional problem into a pair of two-dimensional problems, given by,

$$\lambda\xi^{o}_{zz} + \xi^{o}_{rr} + \xi^{o}_{r}/r = 0 \quad ,$$

$$\xi^{o}_{r}\Big|_{\text{surface}} = dR/dz \quad , \qquad \xi^{o}_{\infty} = 0$$

and

$$\lambda\xi^{1}_{zz} + \xi^{1}_{rr} + \xi^{1}_{r}/r - \xi^{1}/r^{2} = 0 \quad ,$$

$$\xi^{1}_{r}\Big|_{\text{surface}} = 0 \quad , \qquad \xi^{1}_{\infty} = \alpha\ r \quad .$$

As the three dimensional problem has been transformed into two two-dimensional problems it will be about twice as difficult to solve the three-dimensional problem as it is to solve a two-dimensional problem. This represents a considerable improvement over the factor of 30 mentioned in the Introduction.

Reyhner[4] has published a three-dimensional solution of the full potential equation. In his paper he observes that the solution is closely approximated by a constant plus a cosine in the circumferential direction. This result is not surprising in light of the above discussion. The solution is exactly a constant plus a cosine in the circumferential direction for the subsonic and for the supersonic problems and is not far different for the transonic non-linear problem.

---

4. *T. A. Reyhner, "Transonic Potential Flow Around Axisymmetric Inlets and Bodies at Angle of Attack," AIAA Journal, Vol. 15, No. 9, September 1977, pp. 1299-1306.*

The ease with which the linear problem may be solved in three dimensions gives one hope that the transonic problem may be similarly transformed. Fourier transform techniques cannot be carried over directly to the non-linear transonic equation, however. A first requirement for the use of Fourier transform techniques is that the equation to which they are applied must be linear. The transformation of the non-linear term of equation (1) would yield a convolution that would couple the resulting set of differential equations. It is also important to note that a second requirement for the use of Fourier transforms is that the operator to which they are applied must be independent of the choice of where the $\theta = 0$ plane is located. That is, the operator must have complete rotational symmetry in θ.

Fourier transform techniques can be applied indirectly to the solution of the non-linear problem. An iterative approach may be applied numerically to the solution of equation (1). In this approach the derivatives with respect to z which occur in the non-linear term are evaluated from an old iteration of the solution. The remaining two-dimensional system in r and θ is linear and is solved to obtain the potential at the next iteration of the solution on a plane in r and θ. The solution may be obtained in this manner for all of the planes perpendicular to the z axis in the flow field. The process may then be continued through many such iterations, evaluating the z derivatives from the solution at the old iteration and obtaining the solution at the new iteration from the resulting linear equations in r and θ. Such a process, of course, may or may not converge. The linear problems generated, however, are symmetrical in θ and Fourier transform techniques may be applied.

This iterative technique in which the potential is obtained for planes cutting the body axis from known values of the z derivative terms is in close harmony with the physical nature of the flow. An examination of the shadowgraph shown in Figure 1 leaves one with a clear image of the radial nature of the pattern of shocks about the body. The effect of a change in the body geometry is felt far out in the flow field in a radial direction from the cause of the disturbance. The effect in the longitudinal direction is not nearly as great.

One would expect to find this situation modeled in the differential equation that is used to predict transonic flow. The ϕ_{zz} derivative term in equation (1), that couples the potential at any point to the potential at longitudinally neighboring points, is scaled by a small coefficient, $1 - M^2 - M^2 (\gamma + 1) \phi_z$. When the local Mach number is one this coefficient is zero. Since the local Mach number is always near one in transonic flow, this coefficient is always much less than one. Near the body surface the ϕ_{zz} term may be neglected entirely in regions away from corners and other discontinuities. The equation that results when the non-linear term is dropped is called the inner equation and is given by,

$$\phi_{rr} + \phi_r/r + \phi_{\theta\theta}/r^2 = 0 \quad . \tag{2}$$

There is no coupling in the longitudinal direction included in this equation.

The radial propogation of physical influence helps to explain the success of line relaxation schemes such as the one Bailey[3] applied to the solution of the two-dimensional cylindrical problem. The direction of the implicit calculation in this solution is maintained in the radial direction which corresponds to the direction of the major physical coupling. It is also of advantage to make use of this physical coupling in the three-dimensional solution of equation (1). This coupling may be taken advantage of if the line relaxation scheme that Bailey used in two dimensions is developed into a plane relaxation scheme in three dimensions.

The implicit system of equations associated with line relaxation is of tri-diagonal form and may be readily solved. The system of equations associated with plane relaxation will be penta-diagonal in form because of the added coupling between the equations around the body. In such a system there will be non-zero elements on the main diagonal and on four side diagonals. Such a system cannot be solved as directly. A finite Fourier transformation, however, will reduce the three-dimensional penta-diagonal system to a series of two-dimensional tri-diagonal problems.

There is an additional advantage to the use of Fourier transformations. They make natural the use of spectral methods. In a spectral method the potential is expanded in a cosine series,

$$\phi = \xi^0 + \xi^1 \cos(\theta) + \xi^2 \cos(2\theta) + \ldots + \xi^k \cos(k\theta) + \ldots$$

The second partial derivative with respect to θ is then,

$$\phi_{\theta\theta} = -\xi^1 \cos(\theta) - 4\xi^2 \cos(2\theta) - \ldots - k^2 \cos(k\theta) - \ldots$$

Since the coefficients of $\cos(k\theta)$ for k larger than 1 are very small in the transonic problem it is possible to evaluate the θ derivative with very few Fourier components. The necessity of keeping only a few Fourier components implies that only a few grid points need be maintained in θ, as will be shown below. In practice no increase in accuracy, of engineering significance, may be seen between the solutions obtained from grids of 4 and 8 points in the θ direction. In the linear case of low Mach number the coefficients for k larger than 1 are zero and only two grid points are necessary. It would be necessary to use at least 16 grid points to evaluate the second derivative of $\cos(\theta)$ with the usual central difference formula.

The Fourier transformations which are useful in the numerical solution of equation (1) are finite. The finite Fourier transformation of the potential may be written as:

$$\xi^k = \left[\sum_{n=1}^{N} \phi^n \exp\left(2\pi i k n/N\right) \right] / \sqrt{N} \quad .$$

The ξ^k's are the transformed potentials associated with the ϕ^n's given at N equally spaced grid points on a circle around the body. There are as many ξ^k's as there are ϕ^n's. The potential may be obtained from the ξ^k's by applying the inverse transformation:

$$\phi^n = \left[\sum_{k=1}^{N} \xi^k \exp\left(-2\pi i k n/N\right) \right] / \sqrt{N} \quad .$$

Since it is possible to go backward and forward between the transformed and untransformed forms of the potential, the finite Fourier transformation can neither add to nor subtract from the information in the equations. The transformation would be described in linear algebra as a change of basis. It may be written as a matrix operator F whose elements are:

$$f_{k,n} = \exp\left(2\pi i k n\right) \quad .$$

The finite Fourier transformation, written in matrix form, is then

$$\vec{\xi} = F \vec{\phi} \quad .$$

The transformed form of an operator O such as the one that will be obtained from the transonic equation is given by,

$$F\, O\, F^{-1} \quad .$$

Fourier transform techniques are natural for the cylindrical problem. As only a few Fourier terms are needed, the transformations use little computer time and a fast solution algorithm is possible. The problem that creates significant difficulty in the use of the transform method arises in the need to stabilize the iterative process used to solve the transonic problem. Stable schemes can be developed as will be shown.

IV. DIFFERENCE FORMULATION

The difference formulation used to solve the three-dimensional cylindrical transonic problem utilizes Fourier transformations. The algorithm is based on plane relaxation and a spectral method is used in the θ direction. Type dependent differencing, as developed by Murman and Cole[5], is also used. Central differences are used to evaluate the ϕ_{rr} derivatives throughout.

In the following, Δ will be used to imply a difference operator of the type described above. That is, $\Delta_{rr}\phi$ will be used to represent the central difference form for the second derivative of ϕ in the r direction. $\Delta_{zz}\phi$ will imply the use of a central difference formula in subsonic regions and the use of a backward difference formula in supersonic regions. Further, $\Delta_{\theta\theta}\phi$ will imply a spectral evaluation of $\phi_{\theta\theta}$.

Difference equations for the transonic problem then may be written as:

$$\Delta_{rr}\phi + \Delta_{r}\phi/r + \Delta_{\theta\theta}\phi/r^2 = -\lambda\Delta_{zz}\phi \qquad (3)$$

where λ represents the non-linear coefficient $1 - M^2 - M^2 (\gamma + 1) \Delta_z\phi$. One such equation will exist for each grid point in the flow field.

The operator represented by the left hand side of this equation meets all of the criterion necessary for the successful application of Fourier transform techniques. It is both linear and symmetric in θ. An iterative plane relaxation procedure could be applied to the solution of the system of equations of the form shown in equation (3). This procedure could be carried forward by evaluating the right hand sides of these equations from the values of the potential available from the last iteration of the solution, and by then solving the resulting linear system for the potential at the next iteration of the solution. Plane after plane of potentials could be obtained in this manner marching from a point upstream of the shell to a point downstream of the shell until the potential for the entire flow field at the new iteration was known. Unfortunately, the repetition of this process for many iterations does not converge to a stable solution. In order to stabilize the iterative process, however, any term which helps stability may be added to either side of equation (1) if the term will disappear when convergence is reached.

---

5. *E. M. Murman and J. D. Cole, "Calculation of Plane Steady Transonic Flows," AIAA Journal, Vol. 9, No. 1, January 1971, pp. 114-121.*

In a study of convergence it is convenient to consider the iterative process to be a marching process through time. Time then forms a fourth dimension in the problem and the marching process may be analyzed accordingly. Differences between potentials at two consecutive iterations are then considered to be related to a derivative in time. On convergence, by definition, the solution has reached a steady state. In a steady state all time derivatives such as θ_t or mixed spatial and time derivatives such as θ_{zt} will disappear. Any combination of θ_t or θ_{zt} terms may be added to either side of equation (1) if they will help stabilize the iterative procedure. Ballhaus[6] has discussed the effect of θ_{zt} terms as they appear in the time dependent transonic small disturbance equation written in Cartesian coordinates. In the cylindrical problem it has been found necessary to apply a type dependent stabilization process. The addition of a $\Gamma\phi_t$ term to the right hand side of the equation at subsonic points and the addition of a $\Gamma\phi_{zt}$ term to the right hand side of the equation at supersonic points has been found to stabilize the iterative process. The coefficient $\Gamma(r,z)$ is a suitably chosen constant in θ.

A stable scheme to which Fourier transform techniques can be applied may then be based on the difference equations given by:

$$\Delta_{rr}\phi + \Delta_r\phi/r + \Delta_{\theta\theta}\phi/r^2 = -\lambda\Delta_{zz}\phi + \Gamma\Delta_{xt}\phi \quad \text{(supersonic)}$$

and (4)

$$\Delta_{rr}\phi + \Delta_r\phi/r + \Delta_{\theta\theta}\phi/r^2 = -\lambda\Delta_{zz}\phi + \Gamma\Delta_t\phi \quad \text{(subsonic)}$$

In order to see explicitly how convergence is achieved it is necessary to write out the right hand side of equations (4) in detail. The notation that will be used is as follows. The potential at the grid point for which the equation is derived will be written as ϕ. The potential at neighboring points in the z direction will be written as ϕ_+ or ϕ_- for neighbors in the positive or negative z directions respectively. $\phi_=$ will be used to represent the potential at the next nearest neighbor grid point in the negative z direction. Potentials which are evaluated at the last time step (iteration) will be marked with a $\hat{}$. Equations (4) then become:

---

6. *William F. Ballhaus and Harvard Lomax, "The Numerical Simulation of Low Frequency Unsteady Transonic Flow Fields,"* Lecture Notes in Physics, *Vol. 35, pp. 57-63 (1975).*

$$\Delta_{rr}\phi + \Delta_r\phi/r + \Delta_{\theta\theta}\phi/r^2 = -\lambda(\hat{\phi}-2\hat{\phi}_-+\hat{\phi}_=)/\Delta_z^2 + \Gamma[(\phi-\hat{\phi}) - (\phi_- - \hat{\phi}_-)]$$

(supersonic)

and (5)

$$\Delta_{rr}\phi + \Delta_r\phi/r + \Delta_{\theta\theta}\phi/r^2 = -\lambda(\hat{\phi}_+ - 2\hat{\phi} + \phi_-)/\Delta_z^2 + \Gamma(\phi - \hat{\phi}) \quad ,$$

(subsonic)

$$\Gamma(z,r) = 2\text{Max}_\theta(\lambda)/\Delta_z^2 \quad .$$

The non-linear coefficient λ has not been written out. It is always central differenced using the old time step. The coefficient Γ is dependent on the maximum value of λ around the circle of grid points at the current value of r and z. Δ_z gives grid separation.

Equations (5) have been written as they would appear for any evenly spaced grid. The grid actually used was not evenly spaced. A slight modification is necessary to write these equations for a varying grid. This modification will not be presented here. In order to solve these equations the $\Gamma\phi$ term is carried from the right hand side to the left where it becomes part of the implicit system of equations which must be solved. The remaining terms on the right hand side of equations (5) may be evaluated from the solution for the old iteration or from the recently acquired solution on the last plane for the new iteration. The right hand side is thus a known driving term for the linear system on the left hand side. An iterative process, as described above, may then be employed.

Convergence has been found to be monotonic and convergence speed may be increased by over-relaxation, as is used in the line over-relaxation technique. Speed of convergence may be further increased by use of a coarse longitudinal grid for the initial iterations followed by the use of a fine grid when the solution has partially formed. By utilizing these techniques quite reasonable run times, on the order of three minutes, have been achieved for three-dimensional cases on fine grids.

V. DISCUSSION OF RESULTS

The results for computations of the surface pressure coefficient for bodies with circular arc profiles can be seen in Figures 3 and 4. Figure 3 shows a comparison of computed and wind tunnel[7] pressure coef-

---

7. *R. A. Taylor and J. B. McDevitt, "Pressure Distribution at Transonic Speeds for Parabolic-Arc Bodies of Revolution Having Fineness Ratios of 10, 12, and 14," NACA TN-4234, March 1958.*

ficient along the surface of a 1/10 fineness ratio body at zero angle of attack in a Mach number .99 free stream. The location of a shock can be clearly seen just aft of the center of the body.

The solid line shows the results of computations for a body generated by a perfect circular arc. The wind tunnel model, however, was supported from the rear by a sting. The effect of the sting was modeled by attaching a solid cylinder to the body at the location of the sting. The corner at the juncture of the body and this cylinder was faired to reduce the large pressure spike that would have formed at a sharp corner. The resulting computed pressure coefficients are shown by the dashed line in this figure. As the angle of attack is zero in the case shown in Figure 3, the computation is two-dimensional. This same case was computed by Bailey in his earlier two-dimensional work[3] and the results are identical.

Figure 4 shows a comparison of computed and wind tunnel[8] pressures for a slightly more slender body of fineness ratio 1/12. The Mach number in this case was .90 which is too low to allow development of a large supersonic region with strong shocks. The figure is presented to show the result of a three-dimensional computation. For the results shown, the sting was modeled in the same manner as discussed above.

The results presented in these two figures confirm the ability of the three-dimensional code to predict surface pressures over smooth bodies. There is little difference between the nose of a typical artillery shell which is an ogive and the front portion of these circular arc bodies. Artillery shell, however, often exhibit corners, particularly at the junction between the ogive and cylinder portions and between the cylinder portion and the boattail. Strong shocks are formed by the collapse of supersonic regions which are generated by the expansion of the flow over these corners when the shell is flown at a slightly subsonic velocity ($.8 < M < 1$). As discussed in the introduction, the flow pattern generated by the corner at the beginning of the boattail is largely responsible for the critical behavior of the overturning moment. Thus, the accurate treatment of corner flow is of prime consideration.

The ability of the present theory to predict flow over a corner can be seen in Figure 5. Figure 5 shows a comparison of computed surface pressures to wind tunnel[9] experiments for flow over a cone cylinder model at Mach number 1.1. The theory shows reasonable

---

8. *J. B. McDevitt and R. A. Taylor, "Force and Pressure Measurements at Transonic Speeds for Several Bodies Having Elliptical Cross Sections," NACA TN-4362, September 1958.*

9. *W. A. Page, "Experimental Study of the Equivalence of Transonic Flow About Slender Cone-Cylinders of Circular and Elliptic Cross Section," NACA TN-4233, April 1958.*

behavior near the corner of the cone and cylinder sections. In order to achieve these results it was necessary to use care in applying boundary conditions at the body surface. An approach that is often taken in the application of boundary conditions is to use solutions of the simpler inner equation (2) to extrapolate the boundary conditions from the body surface to the body axis or to some other convenient location. In Bailey's two dimensional paper[3] the boundary conditions were extrapolated to the axis where a series of sources and sinks were placed. The source and sink strengths were obtained from the solution to the inner equation (2).

This procedure is not feasible if accurate corner flow is to be obtained. The equation, which is obtained by dropping the non-linear term from equation (1), does not apply near corners where, in fact, the non-linear term may be large close to the body surface. Boundary conditions must be applied directly at the surface without extrapolation.

Additional improvement in the application of boundary conditions for flow over corners may also be obtained as indicated below. The usual boundary condition which is applied at the body surface is given by,

$$\phi_r\Big|_{\text{surface}} = dR/dz \quad ,$$

where the left hand side is the radial derivative of the potential evaluated at the body surface and the right hand side is the slope of the body surface. This is a first order approximation to the body surface boundary condition. A second order formula is more appropriate and is given by,

$$\phi_r\Big|_{\text{surface}} = (1 + \phi_z\Big|_{\text{surface}})\, dR/dz \quad .$$

The first order formula works well as long as ϕ_z remains small in comparison to 1. Near a corner ϕ_z may become large enough that it produces a noticeable effect as seen in Figure 5. Because of the iterative relaxation procedure used in solving the potential equation ϕ_z may be obtained at an old iteration. The right hand side of the second order formula may thus be evaluated. The effect of using a finer grid spacing may also be seen in Figure 5. The grid in all cases shown in this figure was made up of 64 points. In the case labeled fine grid, these points were clustered so as to give twice the density near the corner. Subsequent calculations have been carried out with 128 points so as to achieve this same fine density when more than one corner is present on the body.

It has been shown in the above discussion that the transonic techniques that have been developed will predict flow over both smooth bodies and bodies with corners. It should, therefore, be possible to obtain the solution over a body that closely resembles an artillery shell. The accuracy with which the shock locations may be predicted for a projectile can be seen in Figure 6. The plot shown in this figure gives the pressure distribution along the surface of a projectile like body. This body differs from the M549 projectile shape in that it has a sharp nose and no rotating band. The outline of an actual M549 projectile appears at the bottom of Figure 6. The expansion locations and shock locations are marked with dashed and solid lines respectively about this outline as taken from a shadowgraph[10] of the projectile in flight at M = .91. There is a double shock pattern associated with the collapse of each supersonic region as may be seen along the outline. The second shock is due to the interaction of the first shock and the viscous boundary layer. The boundary layer separates at the base of the first shock and reattaches at the base of the second. Reasonable agreement between the shock locations seen in the computed pressure distribution and the primary shock locations taken from the shadowgraph are seen.

The secondary shock is an effect caused by the viscous boundary layer which is not modeled in the inviscid computations. The presence of the rotating band and the effect of the viscous boundary layer in rounding the corner at the boattail are also not modeled in the computations. Aerodynamic coefficients computed for the projectile like body are not, therefore, expected to be in exact agreement with the aerodynamic coefficients for the actual projectile. The transonic effects can, however, be computed and qualitatively correct behavior can be predicted. The lift loading computed for the projectile shape is plotted in Figure 7. This graph shows the normal force per unit length plotted as a function of the position along the shell. It is felt that the features of this curve, particularly the large downward spike in the boattail region, give an accurate representation of the aerodynamic forces on this body. Comparison of the pitching moment coefficient computed for this body and range measurements[11] of the pitching moment for the M549 projectile are given as a function of Mach number in Figure 8. The peak shown in the computed results falls a few hundredths of a Mach number higher than the peak in the range measurements and is not as pronounced.

The trend of design alterations may be predicted by the present technique. The boattail on the projectile shape discussed above was

---

10. *Leonard C. MacAllister, U.S. Army Ballistic Research Laboratory, Aberdeen Proving Ground, Maryland, shadowgraph taken in BRL Transonic Range.*

11. *Robert L. McCoy, U.S. Army Ballistic Research Laboratory, Aberdeen Proving Ground, Maryland, private communication.*

shortened producing the results seen in Figure 9. The flow over the boattail becomes fully supersonic at a lower Mach number for the shortened tail and transonic effects due to the shocks on the boattail thus disappear at a lower Mach number. This causes the peak in the pitching moment to appear at a lower Mach number.

VI. SUMMARY

In order to compute the aerodynamic coefficients for artillery projectiles it has been necessary to resolve the shock patterns associated with corner flows. This resolution is obtained by using very fine grids and by using care in the application of boundary conditions. A practical computational algorithm has been developed which is based on Fourier transformation techniques and which has been used to solve the transonic small disturbance equation on a cylindrical coordinate system in three dimensions. The ability of these methods to accurately predict transonic flow about clean aerodynamic shapes has been demonstrated by comparisons of the computations to experimental data for circular arc and cone cylinder bodies. The techniques have also been shown to predict the correct qualitative trends of C_{m_α} vs Mach number for actual shell configurations. In order to achieve improved agreement between computed and experimental aerodynamic coefficients for actual shell, it will be necessary to include effects of the viscous boundary layer and to include a model for the rotating band.

Figure 1. Spark Shadowgraph of a Typical Projectile at Critical Mach Number, M = 0.926, α = 8°

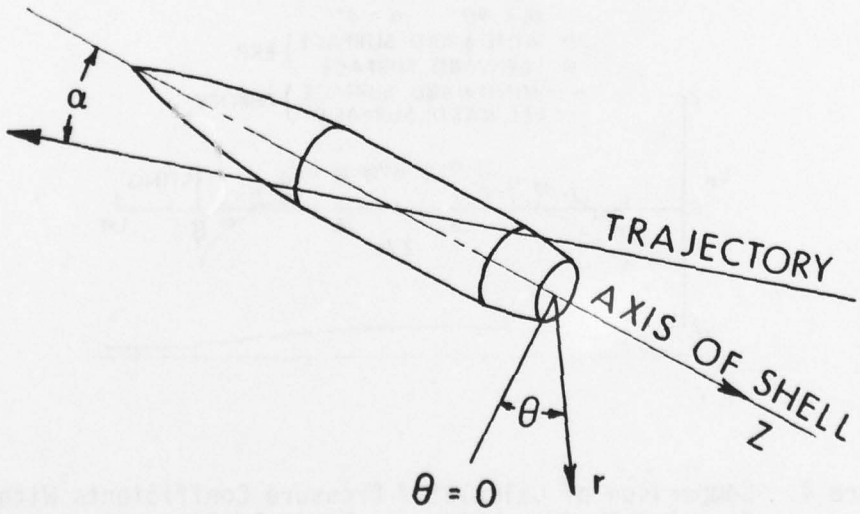

Figure 2. Coordinate System

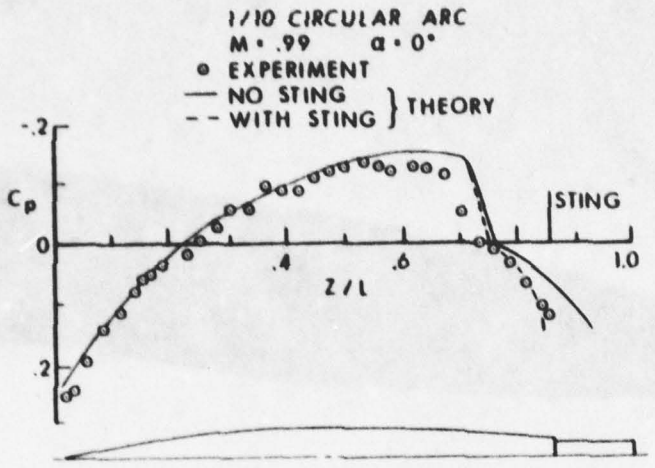

Figure 3. Comparison of Calculated Pressure Coefficients With Wind Tunnel Data for a Fineness Ratio 1/10 Circular Arc Body, M = 0.99

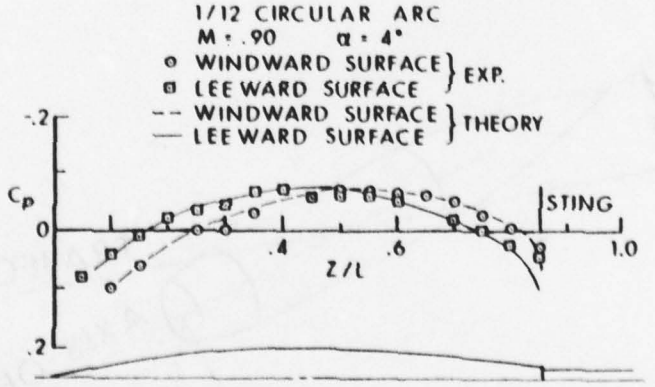

Figure 4. Comparison of Calculated Pressure Coefficients With Wind Tunnel Data for a Fineness Ratio 1/12 Circular Arc Body at Angle of Attack, α = 4°, M = 0.90

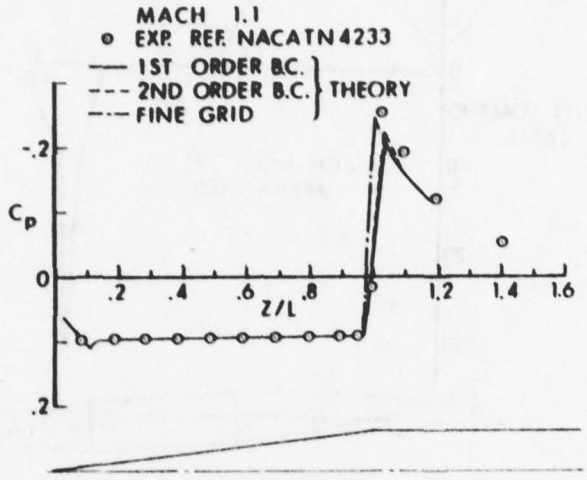

Figure 5. Comparison of Calculated Pressure Coefficient With Wind Tunnel Data for a 7° Half Angle Cone Cylinder, M = 0.99

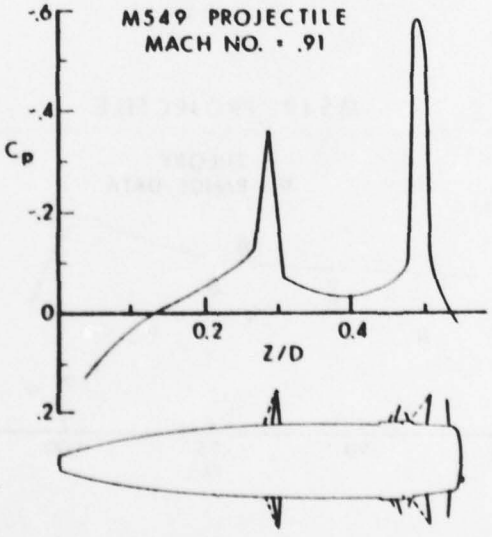

Figure 6. Calculated Surface Pressure Coefficient on an M549 Projectile Shape

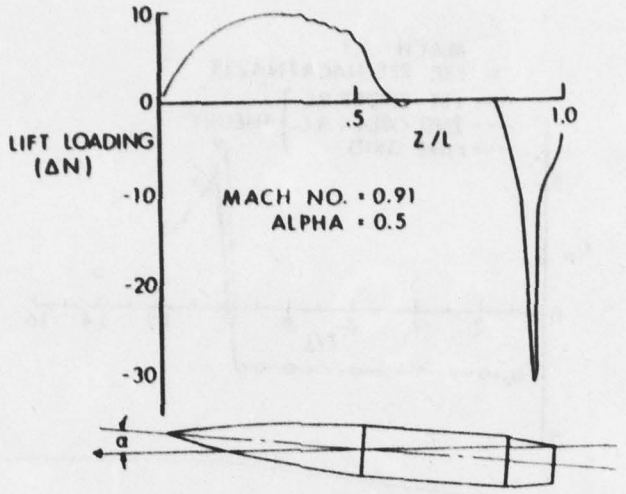

Figure 7. Computed Normal Force Loading Along Modeled M549 Projectile Shape

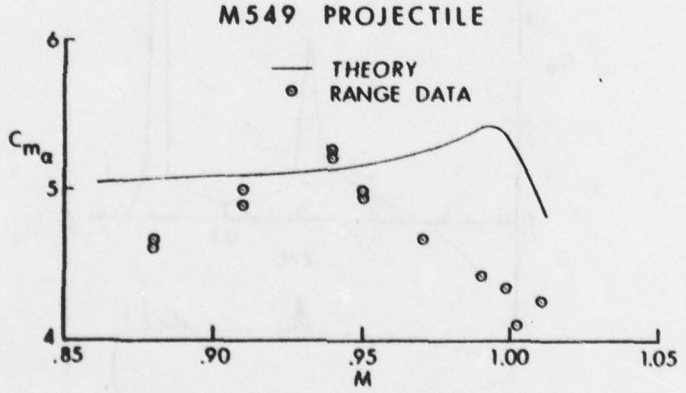

Figure 8. Comparison of Computed Pitching Moment With Range Data for an M549 Projectile

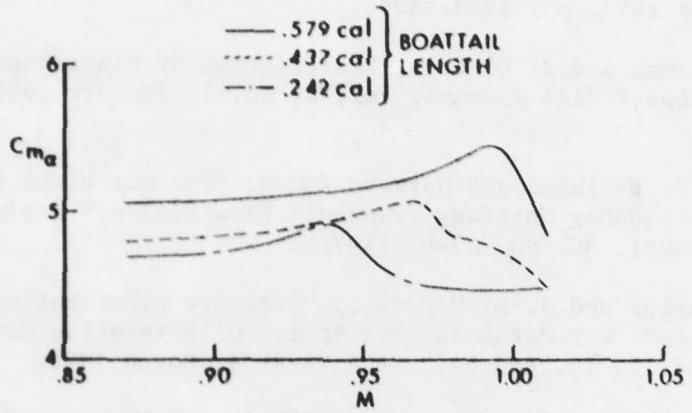

Figure 9. Calculated Pitching Moment as a Function of Mach Number Showing the Trend With a Shortened Boattail

REFERENCES

1. F. R. Bailey and W. F. Ballhaus, "Comparisons of Computed and Experimental Pressures for Transonic Flow About Isolated Wings and Wing Fuselage Configurations," NASA SP-347, Vol. 2, March 1975, pp. 1213-1226.

2. Holt Ashley and Marten Landahl, *Aerodynamics of Wings and Bodies*, Addison-Wesley Publishing, Inc., Reading, MA (1965).

3. F. R. Bailey, "Numerical Calculation of Transonic Flow About Slender Bodies of Revolution," NASA TN-D-6582, December 1971.

4. T. A. Reyhner, "Transonic Potential Flow Around Axisymmetric Inlets and Bodies at Angle of Attack," *AIAA Journal*, Vol. 15, No. 9, September 1977, pp. 1299-1306.

5. E. M. Murman and J. D. Cole, "Calculation of Plane Steady Transonic Flows," *AIAA Journal*, Vol. 9, No. 1, January 1971, pp. 114-121.

6. William F. Ballhaus and Harvard Lomax, "The Numerical Simulation of Low Frequency Unsteady Transonic Flow Fields," *Lecture Notes in Physics*, Vol. 35, pp. 57-63 (1975).

7. R. A. Taylor and J. B. McDevitt, "Pressure Distribution at Transonic Speeds for Parabolic-Arc Bodies of Revolution Having Fineness Ratios of 10, 12, and 14," NACA TN-4234, March 1958.

8. J. B. McDevitt and R. A. Taylor, "Force and Pressure Measurements at Transonic Speeds for Several Bodies Having Elliptical Cross Sections," NACA TN-4362, September 1958.

9. W. A. Page, "Experimental Study of the Equivalence of Transonic Flow About Slender Cone-Cylinders of Circular and Elliptic Cross Section," NACA TN-4233, April 1958.

10. Leonard C. MacAllister, U.S. Army Ballistic Research Laboratory, Aberdeen Proving Ground, Maryland, shadowgraph taken in BRL Transonic Range.

11. Robert L. McCoy, U.S. Army Ballistic Research Laboratory, Aberdeen Proving Ground, Maryland, private communication.

LIST OF SYMBOLS

$C_{m\alpha}$	pitching moment coefficient about center of mass
C_p	pressure coefficient
$f_{k,n}$	matrix element of F
F	Fourier transformation matrix
k	index associated with Fourier components (wave number)
M	Mach number
n	index associated with grid location in θ direction
N	total number of grid points in θ direction
O	arbitrary matrix operator
r	radial coordinate
R	radius of body
z	longitudinal coordinate
α	angle of attack
γ	ratio of specific heats (1.4)
Γ	coefficient of time derivative term
Δ	difference operator
ΔN	lift loading
θ	circumferential angular coordinate
λ	non-linear coefficient
ν	transformed potential
ξ^k	k'th Fourier component
ϕ	perturbation velocity potential

DISTRIBUTION LIST

No. of Copies	Organization
12	Commander Defense Documentation Center ATTN: DDC-DDA Cameron Station Alexandria, VA 22314
1	Commander US Army Materiel Development and Readiness Command ATTN: DRCDMD-ST, N. Klein 5001 Eisenhower Avenue Alexandria, VA 22333
1	Commander US Army Aviation Research and Development Command ATTN: DRSAV-E P. O. Box 209 St. Louis, MO 63166
1	Director US Army Air Mobility Research and Development Laboratory Ames Research Center Moffett Field, CA 94035
1	Commander US Army Electronics Research and Development Command Technical Support Activity ATTN: DELSD-L Fort Monmouth, NJ 07703
1	Commander US Army Communications Research and Development Command ATTN: DRDCO-PPA-SA Fort Monmouth, NJ 07703
1	Commander US Army Jefferson Proving Ground ATTN: STEJP-TD-D Madison, IN 47250
3	Commander US Army Missile Research and Development Command ATTN: DRDMI-R DRDMI-RDK Mr. R. Deep Mr. R. Becht Redstone Arsenal, AL 35809
1	Commander US Army Missile Materiel Readiness Command ATTN: DRSMI-AOM Redstone Arsenal, AL 35809
1	Commander US Army Tank Automotive Research & Development Command ATTN: DRDTA-UL Warren, MI 48090
8	Commander US Army Armament Research and Development Command ATTN: DRDAR-TSS (2 cys) DRDAR-LCA-F Mr. D. Mertz Mr. E. Falkowski Mr. A. Loeb Mr. R. Kline Mr. S. Kahn Mr. S. Wasserman Dover, NJ 07801
1	Commander US Army Armament Materiel Readiness Command ATTN: DRSAR-LEP-L, Tech Lib Rock Island, IL 61299
1	Director US Army TRADOC Systems Analysis Activity ATTN: ATAA-SL, Tech Lib White Sands Missile Range NM 88002

DISTRIBUTION LIST

No. of Copies	Organization
1	Arnold Research Organization, Inc. von Karman Gas Dynamics Facility ATTN: Dr. John C. Adams, Jr. Aerodynamics Division Projects Branch Arnold AFS, TN 37389
1	Commander US Army Research Office P. O. Box 12211 Research Triangle Park NC 27709
1	Commander US Naval Surface Weapons Center ATTN: Code 312 Mr. S. Hastings Silver Spring, MD 20910
4	Director NASA Ames Research Center ATTN: MS 202-1 Dr. F. R. Bailey Dr. W. F. Ballhaus MS 229-1, Dr. J. Rakich MS 202, Tech Lib Moffett Field, CA 94035
3	Director NASA Langley Research Center ATTN: MS-185, Tech Lib MS-163, Dr. D. Bushnell MS-360, Dr. J. South Langley Station Hampton, VA 23365
1	Nielsen Engineering and Research, Inc. ATTN: Dr. Stephen S. Stahara 510 Clyde Avenue Mountain View, CA 94043
1	Rockwell International Science Center ATTN: Dr. N. Malmuth 1049 Camino Dos Rios P. O. Box 1085 Thousand Oaks, CA 91360
1	Princeton University James Forrestal Research Center Gas Dynamics Laboratory ATTN: Dr. D. Dolling Princeton, NJ 08540
1	University of Delaware Mechanical and Aerospace Engineering Department ATTN: Dr. J. E. Danberg Newark, DE 19711
	Aberdeen Proving Ground
	Director, USAMSAA ATTN: Dr. J. Sperrazza DRXSY-MP, H. Cohen Cdr, USATECOM ATTN: DRSTE-SG-H